Dinamika Teknik Mesin 13(2) (2023) 173-179

Dinamika Teknik Mesin
Jurnal Keilmuan dan Terapan Teknik Mesin
http://dinamika.unram.ac.id/index.php/DTM/index

Design and optimization of a simple atmospheric water generator using a thermoelectric module

T.A. Ajiwiguna*, M.R. Kirom
Engineering physics study program, Telkom University, Jalan Telekomunikasi Terusan Buah Batu, Bandung, Indonesia.
*E-mail: triayodha@telkomuniversity.ac.id

ARTICLE INFO

Article History:
Received 03 July 2023
Accepted 30 September 2023
Available online 01 October 2023

Keywords:
Atmospheric water generator
Thermoelectric
Surface area
Water production

ABSTRACT

Atmospheric water generator (AWG) is a device for producing water from humid air. The water is produced by cooling the air until below its dew point temperature. This study presents the optimization of a simple thermoelectric AWG device (S-TEAWG) for emergency purposes. The designed S-TEAWG consists of a thermoelectric module and condensation plate as a cooler and condensation surface, respectively. The plate is attached to the cold side of the thermoelectric module to enhance the contact surface area with the ambient air. The thermoelectric module with the dimension of 4 cm × 4 cm is operated at 12 V of voltage and 50°C of hot side temperature. The device is installed vertically thus the condensates flow down naturally due to gravity. Various surface areas of vertical plates, from 0.01 m^2 to 0.09 m^2, are evaluated theoretically to obtain the maximum water production. The results show that the lower temperature of the vertical plate is achieved at a smaller surface area. However, the optimum surface area is obtained at 0.03 m^2 with 60.9 ml/d of water production.

Dinamika Teknik Mesin, Vol. 13, No. 2, Oktober 2023, ***p. ISSN: 2088-088X, e. ISSN: 2502-1729***

1. INTRODUCTION

In certain conditions such as in remote areas, the availability of water is very limited. One of the common solutions for water scarcity is desalination which produces fresh water from seawater or brackish water. Many desalination techniques have been introduced such as reverse osmosis, distillation, membrane distillation, etc (Bundschuh et al., 2021; Nassrullah et al., 2020; Qasim et al., 2019). However, those techniques require saline water as a feed. In some cases, where the feed water is not available, other techniques are needed. Capturing water from the humid air is one of the alternative solutions to this condition. The device to do so is called the atmospheric water generator (AWG). The water vapour contained in the air can be condensed into water by cooling the air until below its dew point temperature. Therefore, the cooling system needed is the AWG.

To create low temperatures, a refrigeration system is needed. Currently, the AWG device usually has a vapour compression or thermoelectric cooling system as its cooler (Avhad et al., 2021; Kadhim et al., 2020; Ramya M and Roopa M, 2020; Vas et al., 2020). The thermoelectric cooling system has several advantages as the refrigeration system compared with the vapor compression system. Thermoelectric technology offers a simpler system, no moving parts, and no need for refrigerant as working fluid. Therefore, it is more compact,

https://doi.org/10.29303/dtm.v13i2.663

lighter, and environmentally friendly. The use of thermoelectric technology for atmospheric water generators has been studied by Joshi et al. (2017). This study resulted in 200 ml of fresh water in 10 hours by utilizing ten Peltier modules with the humidity of ambient air at 80%. Since their design was a complex system, it was not suitable for emergency purposes. Offir et al. (2020) developed the AWG system and reported that the produced water was potable. This study presents the evaluation of the performance of a simple thermoelectric atmospheric water generator device (S-TEAWG). The system is designed as simple as possible because it is used for emergency devices. The optimization of the system is also performed theoretically by investigating the condensation surface area.

2. SYSTEM DESCRIPTION

Figure 1 shows the system of the S-TEAWG which consists of the thermoelectric module (TEM), copper plate, heat sink, and fan. The thermoelectric module is operated at a constant voltage of 12 V supplied by a DC power supply and the hot side is maintained at 50^{o}C by employing a heat sink and fan. The copper plate with a thickness of 0.2 mm is attached to the cold side of the thermoelectric module as the condensation surface.

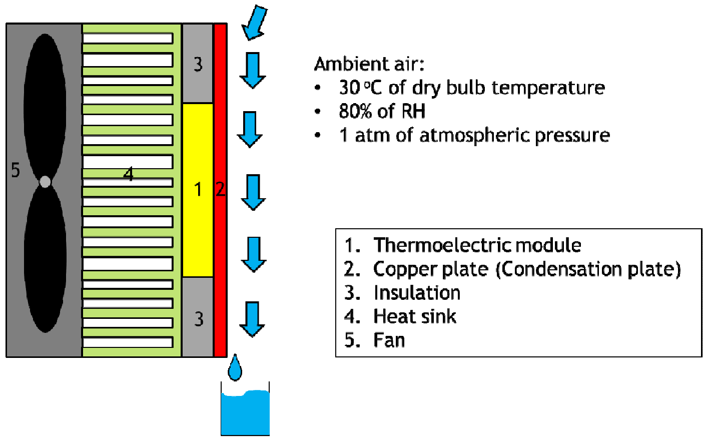

Figure 1. Schematic of compact thermoelectric atmospheric water generator device (S-TEAWG)

Once the thermoelectric module is turned on, the temperature at the cold side of TEM is decreased dramatically due to the heat absorption rate from TEM. This heat absorption rate also decreases the temperature of the copper plate. If the temperature of the copper plate achieves the dew point temperature, the condensates are formed on the surface of the copper plate. Then, condensates flow down due to gravity forces and are collected in the water collector as the products.

Since the copper plate temperature is lower than ambient temperature, natural convection occurs between them. This phenomenon creates downward airflow which acts as a feed humid air for the water generator. The lower copper plate area makes less thermal load, thus lower temperature is achieved and causes more condensation. However, the less copper plate area also makes a smaller contact area between the condensation surface and ambient air. Thus, the condensate production is also lower. To obtain the maximum water production, the area of the copper plate should be optimized. Various surface areas of copper plate are tested from 0.01 m^2 to 0.09 m^2.

3. METHODS

The overall procedures for estimating the water (condensate) production by using S-TEAWG are shown in Figure 2. First, the TEM performance is evaluated by using technical data issued by the manufacturer, Ajiwiguna et al. (2018). Second, the heat transfer rate between certain areas of condensation surface and ambient air is evaluated by using the empirical equation for the vertical surface. Third, a function of surface temperature dependence on the cold side temperature of TEM is characterized by the empirical equation of spreading thermal resistance, Lee et al. (1995). Once, the three functions from the previous steps are obtained, the operating temperature of the condensation surface, cold side temperature of TEM, and heat absorbed rate by the system are determined. Then, the airflow adjacent to the condensation surface is estimated. Finally, the condensate rate production is then estimated by psychrometric analysis.

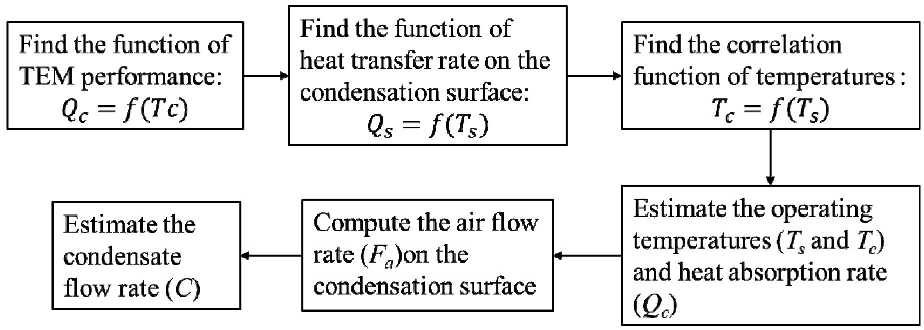

Figure 2. Flowchart of condensate flow estimation method

3.1 TEM performance evaluation

The performance of TEC was evaluated based on the technical data issued by the manufacturers. Table 1 shows the important parameters of the TEC if the hot side temperature of the device is operated at 50°C. These parameters were then used to estimate the thermoelectric properties, Seebeck coefficients (α), thermal resistance (θ), and electrical resistance (R), by using equations 1, 2, and 3 respectively, Ajiwiguna et al. (2018).

Table 1. Important parameters of thermoelectric cooler issued by the manufacturer.

No	Parameter	Value
1	T_H	50°C
2	ΔT_{max}	75°C
3	Q_{max}	57 W
4	I_{max}	6.4 A
5	V_{max}	14.4 V

$$\alpha = \frac{V_{max}}{T_H} \tag{1}$$

$$\theta = \frac{\Delta T_{max}}{I_{max}} \frac{2T_H}{(T_H - \Delta T_{max})} \tag{2}$$

$$R = \frac{V_{max}}{I_{max}} \frac{(T_H - \Delta T_{max})}{T_H} \tag{3}$$

where T_H, ΔT_{max}, I_{max}, and V_{max} are the hot side temperature of TEC, the maximum temperature difference between the cold side and hot side of TEC, the current to achieve ΔTmax, and the voltage to achieve ΔT_{max} respectively.

The TEC module was operated at a constant voltage of 12 V and a hot side temperature of 50°C. Once the thermoelectric properties above were obtained, the heat absorption by the cold side of TEC (Qabs) was estimated by equations 4 and 5, Ajiwiguna et al. (2018).

$$\dot{Q}_{abs} = I\alpha T_c - \frac{(T_H - T_c)}{\theta} - \frac{1}{2} I^2 R \tag{4}$$

$$I = \frac{V - \alpha \Delta T}{R} \tag{5}$$

By varying the cold side temperature and following the above procedure, the characteristic of the TEC module is obtained in the simple equation below, which is the simple function correlation between Qabs and Tc.

$$\dot{Q}_{abs} = f(T_c) \tag{6}$$

https://doi.org/10.29303/dtm.v13i2.663

3.2 Heat convection rate evaluation on condensation surface

The vertical plate was used as the condensation surface. Since the condensation surface temperature was lower than ambient, natural convection heat transfer occurred between the surface and ambient air. The heat transfer rate ($\dot{Q}_{conv}$) was calculated by using equations 6 to 10, Cengel (1997).

$$\dot{Q}_{conv} = h\,A\,(T_s - T_a) \tag{7}$$

$$h = \frac{k\,Nu}{L_c} \tag{8}$$

$$Nu = 0.59\,Ra^{0.25} \tag{9}$$

$$Ra = \frac{g\,\beta\,L_c^3\,(T_s - T_a)}{\nu^2}Pr \tag{10}$$

where h is convection heat transfer coefficient, A is contact area between air and surface, T_s is surface temperature, T_a is ambient air, k is thermal conductivity of air, Nu is Nusselt number, L_c is characteristic length, Ra is Rayleigh number, g is gravity acceleration, β is expansion coefficient, ν is kinematic viscosity, and Pr is Prandtl number.

The heat transfer rate was calculated with variations in surface temperature. Thus, the function of heat transfer rate with the surface temperature was obtained. The simple function is expressed by equation 11.

$$\dot{Q}_{conv} = f(T_s) \tag{11}$$

3.3 Heat transfer analysis on the S-TEAWG

S-TEAWG used the cooling effect of the thermoelectric module. Since the temperature of the cold side is lower than ambient, the heat is transferred from the ambient to the cold side of TEM. The analogy of heat transfer rate to the electrical circuit is shown in Figure 3. The heat is absorbed by the cold side of TEM through three thermal resistances. Since the surface area of the TEM cold side was different from the condensation surface, the spreading thermal resistance was evaluated between them. The method introduced by Lee et al. (1995) was used for the spreading thermal resistance (Rsp) calculation. The conduction thermal resistance (Rcond) and convection thermal resistance (Rconv) were calculated by using equations 12 and 13, respectively.

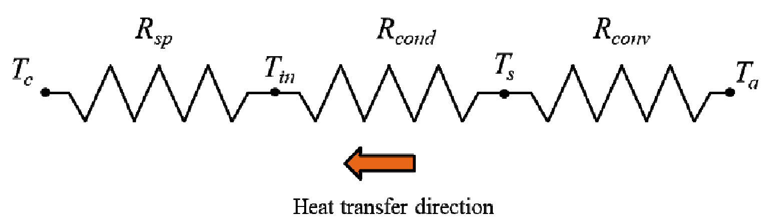

Figure 1. Heat transfer process on the S-TEAWG in the form of electric circuit analogy

$$R_{cond} = \frac{L_p}{k\,A_s} \tag{12}$$

$$R_{conv} = \frac{1}{h\,A_s} \tag{13}$$

where L_p is the thickness of the condensation plate, k is the thermal conductivity of the condensation plate, h is the coefficient of convection of natural convection between the condensation surface and ambient, and A_s is the surface area of the condensation surface. Once all the thermal resistances were obtained, the heat transfer rate on the system ($\dot{Q}$) can be calculated by using equations 14 and 15.

$$\dot{Q} = \frac{(T_a - T_c)}{R_{tot}} \tag{14}$$

$$R_{tot} = R_{sp} + R_{cond} + R_{conv} \tag{15}$$

By using the above analogy, the heat transfer rate on the system$(\dot{Q})$, heat convection ($\dot{Q}_{conv}$), and heat absorbed by TEM ($\dot{Q}_{abs}$) were the same. Therefore, the operating temperatures and heat transfer rate were obtained by combining equation 14, 11, and 6. To estimate the condensation rate (water production), the psychrometric analysis was conducted as explained in the next step.

3.4 Condensation flow rate estimation

The condensation mass flow rate ($\dot{m}_c$) is the produced water by S-TEAWG. To estimate the condensation rate, the air mass flow rate ($\dot{m}_a$) adjacent to the condensation surface was first calculated by using equation 16, Engineering ToolBox (2005).

$$\dot{m}_a = \rho\left(0.019\left(g\,\frac{(T_{amb}-T_s)}{(273+T_{amb})}\right)^{0.4} L_c^{1.2}\right)W \quad (16)$$

where W and ρ are the width of the condensation surface and the density of air, respectively. Then, by using psychrometric analysis, the ratio humidity of the air before and after passing through the condensation surface was known. Equation 17 was then used to estimate the condensation rate ($\dot{m}_c$) from the surface.

$$\dot{m}_c = \dot{m}_a(w_{in} - w_{out}) \quad (17)$$

where w_{in} and w_{out} are the ratio humidity of air before and after passing through the condensation surface.

4. RESULT AND DISCUSSION

Figure 4 shows the correlation between the cold side temperature of the TEC module and heat absorbed by the system. The blue solid line was obtained by analyzing the TEC module performance. The lower cold side temperature can be achieved on the lower thermal load which is represented by the heat absorption rate. Meanwhile, the yellow solid line was obtained from the heat transfer analysis on the S-TEAWG system for a 0.04 m^2 area of condensation surface. Naturally, the lower cold side temperature created a lower temperature of condensation surface, Cengel (1997). However, it also resulted in higher temperature differences between the condensation surface and ambient air. Therefore, the heat convection between them became higher. The operating temperature and heat absorption rate were estimated by finding the intersection of the two lines. In this case, 0.04 m^2 condensation surface, the operating temperature of the cold side of TEC was obtained at -7.15 ^{o}C with a heat absorption rate of 4.66 W. Once the operating temperature of the cold side of the TEC module, the temperature of condensation surface was estimated by analyzing the heat transfer rate on the system, which was obtained at 5.4 ^{o}C. Then, by using equations 16 and 17, the condensation rate was obtained at 2.4 ml/d.

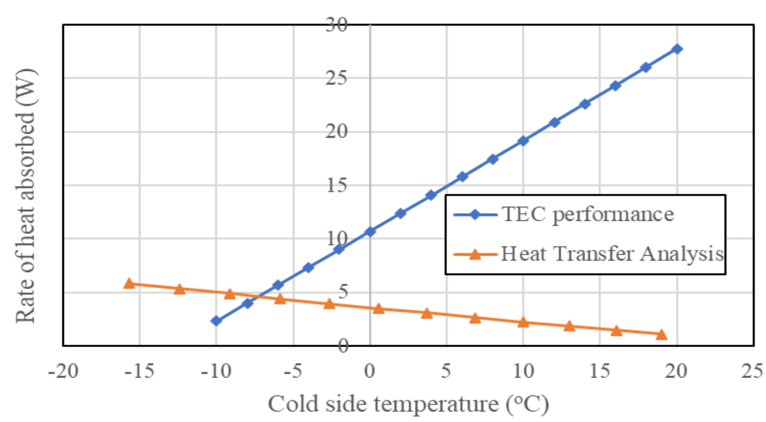

Figure 2. Correlation of cold side temperature and heat absorption rate on the S-TEAWG

By using the same procedure above, the variation of condensation surface area resulted in different operating temperatures, as shown in Figure 5. The operating temperature of condensation surface area tended to be increased with a larger surface area. The larger surface area created a higher heat absorption rate. The heat transfer phenomenon between the condensation surface and ambient air was convection heat transfer, which is proportional to the surface area and temperature difference between the surface and ambient air. As a result, the temperature difference between the condensation surface and ambient air was smaller on the larger condensation surface area.

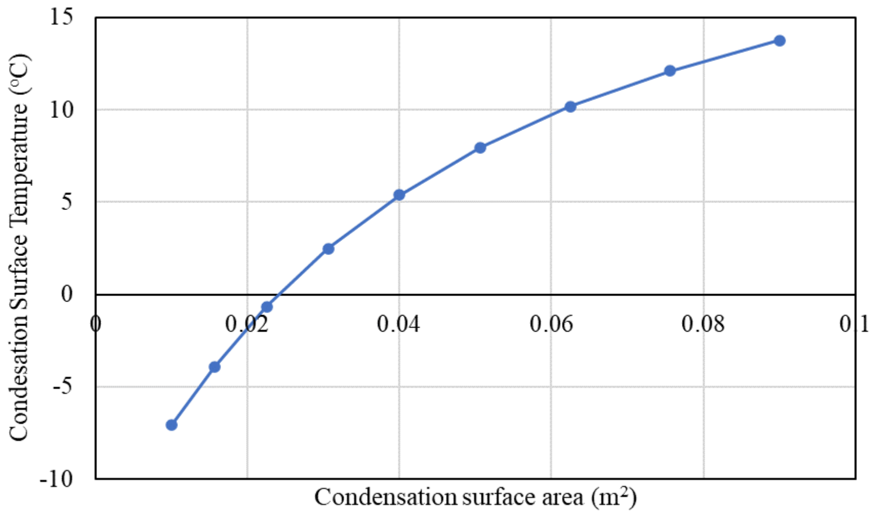

Figure 3. Correlation of the area and operating temperature of condensation surface area

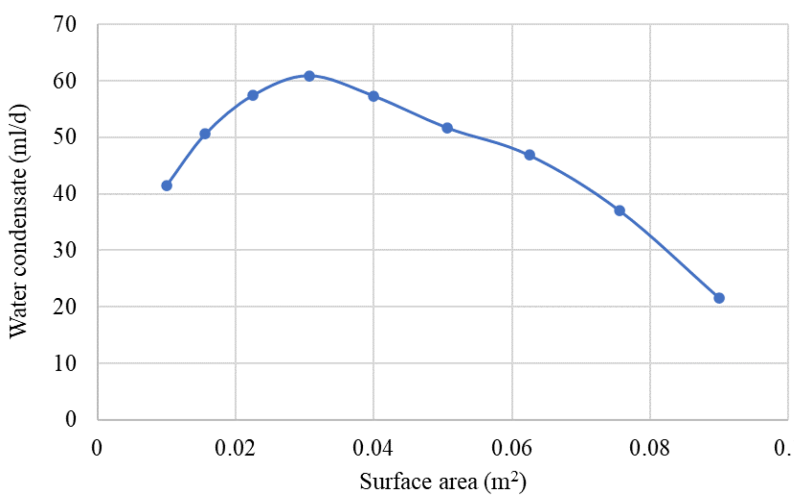

Figure 4. Condensation rate with different surface area

The effect of condensation surface area on the condensation rate is shown in Figure 6. These results were obtained procedurally starting from estimating the operating temperature of the condensation surface (equations 11 and 14) to the estimated condensation rate (equation 17). The optimum surface was obtained at 0.03 m2 with the condensation rate at 60.9 ml/d. The smaller surface area can achieve lower temperatures, but condensation also occurs in smaller areas. Therefore, the condensation rate is lower than the optimum area. On the other hand, the larger surface area created higher temperature which created a lower condensation rate as well. The previous study harvested 200 ml in 10 hours of operation with 10 TEM, Joshi et al. (2017). Shanshan et al. (2017) reported that their device produced 251 ml for ten hours of operation using electric power at 58.2 W. Meanwhile, the estimated harvested water of the proposed S-TEAWG in the same operation hours and conditions was 253 ml. The other study claimed that harvested water was at 600 ml/h using four TEMs in the system, Sri

Suryaningsih and Otong Nurhilal (2016). It implied that the result of S-TEAWG was reasonable with a simple system.

5. CONCLUSION

The simple thermoelectric atmospheric water generator (S-TEAWG) was theoretically investigated in this study. The device consisted of one thermoelectric module, a heatsink and fan, and a condensation plate. The condensation plate was cooled due to the Peltier effect from the thermoelectric module. The condensation occurred on the condensation plate because the temperature was below the dew point. The TEM was operated at a constant voltage of 12 V and a constant hot side temperature of 50^{o}C. To obtain the optimum condition, the S-TEAWG was evaluated with different condensation plate areas ranging from 0.01 m^2 to 0.09 m^2. The optimum condition was achieved at 0.03 m^2 of condensation surface area with the rate of condensate production at 60.9 ml/d.

REFERENCES

Ajiwiguna, T.A., Nugroho, R., Ismardi, A., Method for thermoelectric cooler utilization using manufacturer's technical information. AIP Conference Proceedings, 1941, 2018.

Avhad, S., Dandekar, A., Chandak, A., Kajale, P., Gohel, N. S, Theoretical Analysis of Atmospheric Water Generator using Thermoelectric Cooler. Proceeding of the Yukhti, 2021.

Bundschuh, J., Kaczmarczyk, M., Ghaffour, N., Tomaszewska, B, State-of-the-art of renewable energy sources used in water desalination: Present and future prospects. Desalination, 508, 2021.

Cengel, Y.A, Heat transfer a practical approach, Mcgraw-Hill, 1997.

Engineering ToolBox, Convective Heat Transmission - Air Velocity and Air Flow Volume. https://www.engineeringtoolbox.com/convective-air-flow-d_1006.html, 2005.

Joshi, V.P., Joshi, V.S., Kothari, H.A., Mahajan, M.D., Chaudhari, M.B., Sant, K.D, Experimental Investigations on a Portable Fresh Water Generator Using a Thermoelectric Cooler. Energy Procedia, 109, 161–166, 2017.

Kadhim, T. J., Abbas, A. K., Kadhim, H.J, Experimental study of atmospheric water collection powered by solar energy using the Peltier effect. IOP Conference Series: Materials Science and Engineering, 671(1), 2020.

Lee, S., Song, S., Au, V., Moran, K.P, Constriction/spreading resistance model for electronics packaging. Proceedings of the 4th ASME/JSME Thermal Engineering Conference, 4, 199–206, 1995.

Nassrullah, H., Anis, S. F., Hashaikeh, R., Hilal, N, Energy for desalination: A state-of-the-art review. Desalination, 491, 2020.

Offir Inbar, Igal Gozlan, Stanislav Ratner, Yaron Aviv, Roman Sirota, Dror Avisar, Producing safe drinkingwater using an atmospheric water generator (AWG) in an urban environment, Water 12, 2940, 2020.

Qasim, M., Badrelzaman, M., Darwish, N. N., Darwish, N. A., Hilal, N, Reverse osmosis desalination: A state-of-the-art review. Desalination, 459(February), 59–104, 2019.

Ramya M, Roopa M. Atmospheric water generator using peltier device, International Journal of Engineering Research & Technology, 8(13), 182–185, 2020.

Shanshan, L., Wei, H., Dengyun, H., Song, L., Delu Chen, Xin Wu, Fusuo Xu, Sijia Li, Experiment analysis of portable atmospheric water generator by thermoelectric cooling method, Energy Procedia 142, 1609–1614, 2017.

Sri Suryaningsih, Nurhilal, O., Optimal design of an atmospheric water generator (AWG) based on the thermo-electric cooler (TEC) for drought in rural, AIP Conference Proceedings 1712, 030009, 2016.

Vas, A. C., Ibnu Masood, B., Ahamad, F., Portable atmospheric water generator, International Research Journal of Engineering and Technology, 1649–1652, 2020.

https://doi.org/10.29303/dtm.v13i2.663